

Engineering Notes

ENGINEERING NOTES are short manuscripts describing new developments or important results of a preliminary nature. These Notes cannot exceed 6 manuscript pages and 3 figures; a page of text may be substituted for a figure and vice versa. After informal review by the editors, they may be published within a few months of the date of receipt. Style requirements are the same as for regular contributions (see inside back cover).

Computational Method for Screened Two-Dimensional Wind Tunnel Inlets

W.J. Coirier* and M.B. Bragg†
Ohio State University, Columbus, Ohio

Nomenclature

$C_{p, \text{wall}}$	= wall pressure coefficient
d	= screen wire diameter
k	= head loss coefficient
L	= inlet length
$M_{ts, \text{ref}}$	= test section reference Mach number
N	= dummy-dependent variable for Poisson system inversion
P	= static pressure or source term in Eq. (5)
P_t	= total pressure
Q_{corr}	= dynamic pressure uniformity parameter
q	= dynamic pressure
Re_d	= local Reynolds number based on screen wire diameter
S	= stream function
u_e	= velocity at exit plane of inlet
X_1	= leading screen location
Y_w	= local distance from inlet centerline to wall

Theoretical Development

THE present method uses the property of constant total head levels on the streamlines of an incompressible inviscid flow to predict screened subsonic wind tunnel inlet flowfields. For a two-dimensional flow, the variation of the total head H_s in a direction normal to the fluid streamlines can be obtained from the X and Y momentum equations and is expressed as¹

$$\frac{\partial H_s}{\partial n} = (u^2 + v^2)^{1/2} \left(\frac{\partial u}{\partial y} - \frac{\partial v}{\partial x} \right) \quad (1)$$

where u and v are the Cartesian velocity components. The total head is related to the pressure, density, and velocity as

$$H_s = P/\rho + 1/2(u^2 + v^2) \quad (2)$$

The existence of the stream function S , from which the velocity field is described as

$$u = \frac{\partial S}{\partial y} \quad (3)$$

$$v = -\frac{\partial S}{\partial x} \quad (4)$$

directly satisfies continuity. Introducing S along with Eqs. (3) and (4) into Eq. (1) and manipulating the resulting source term, the following Poisson equation results¹:

$$S_{xx} + S_{yy} = \frac{\partial H_s}{\partial S} \quad (5)$$

where $\partial H_s / \partial S$ is defined as the source term $P(S)$.

The introduction of turbulence management devices into the inlet flowfield can cause total head variation from streamline to streamline, which can be directly related to the source term $P(S)$ in Eq. (5). The head loss on a streamline as it passes through a turbulence screen has been thoroughly investigated,^{2,3} resulting in various empirical models relating a head loss coefficient k to the screen porosity β (open/total area) and the local Reynolds number based on screen diameter Re_d . On a given streamline, the total effective head loss experienced in passing through m screens can be expressed as

$$\Delta H_{s, \text{eff}} = \sum_{m=1}^m k(\beta, Re_d) \frac{u^2}{2} \quad (6)$$

If the flow upstream of the turbulence management devices is at a uniform total head level, the source term in Eq. (5) can then be expressed as

$$P(S) = -\frac{\partial}{\partial S} (\Delta H_{s, \text{eff}}) \quad (7)$$

The determination of the screen-induced rotational inlet flowfield is now reduced to solving Eq. (5) with the source term expressed as in Eq. (7). Using current solution techniques, one may solve Eq. (5) by generating a grid network in the physical domain (inlet) and by then solving the transformed version of Eq. (5) on the rectangular computational domain.

The present method uses the similarity of Eq. (5) as one of the components of the classic Poisson system of elliptic grid-generation equations. Introducing a Laplace equation of a different dependent variable N as

$$N_{xx} + N_{yy} = 0 \quad (8)$$

Received Dec. 4, 1986; revision received Jan. 16, 1987. Copyright © American Institute of Aeronautics and Astronautics Inc., 1987. All rights reserved.

*Graduate Research Associate, Department of Aeronautical and Astronautical Engineering (presently, Research Scientist, Propulsion Gas Dynamics Division, Science Applications International Corporation, Princeton, NJ). Member AIAA.

†Assistant Professor, Department of Aeronautical and Astronautical Engineering, Senior Member AIAA.

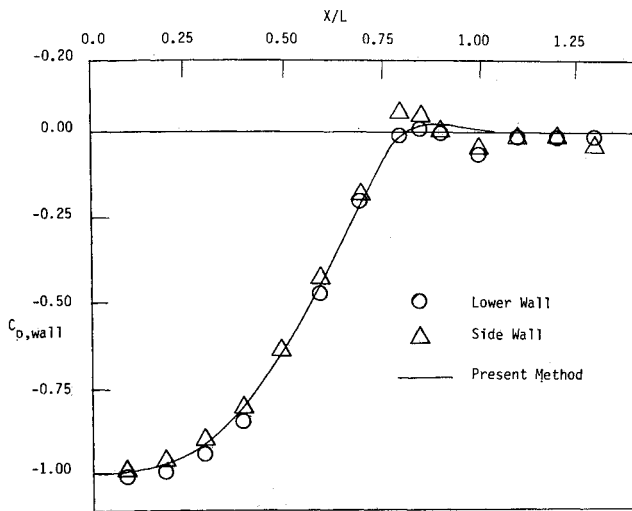


Fig. 1 Measured and predicted wall pressure coefficients.

and inverting the Poisson system [Eqs. (5) and (8)] exchanges the roles of the dependent and independent variables. The following elliptic partial differential equations resulting from this inversion are solved on the rectangular computational domain:

$$AX_{ss} - 2B X_{sn} + CX_{nn} = -J^2(PX_s) \quad (9)$$

$$AY_{ss} - 2B Y_{sn} + CY_{nn} = -J^2(PY_s) \quad (10)$$

$$A = X_n^2 + Y_n^2 \quad (11)$$

$$B = X_s X_n + Y_s Y_n \quad (12)$$

$$C = X_s^2 + Y_s^2 \quad (13)$$

$$J = X_s Y_n - X_n Y_s \quad (14)$$

These equations determine the X and Y locations of lines of constant S (streamlines) and constant N on the physical domain (inlet). Since the transformation yields the flow streamlines, generation of the grid directly yields the velocity field in the inlet.

Equations (9) and (10) were solved numerically by the use of finite differences. The spatial derivatives were discretized using second-order central and one-sided differences and the equations were solved using a successive line-relaxation method.¹ The boundary conditions on the transformed (rectangular) computational domain correspond to defining the value of the stream function S on the upper and lower boundaries and the flow angle at the inflow and outflow planes. To evaluate the head losses to form $P(S)$ in Eq. (5), the velocity field at each screen plane is evaluated during each iteration cycle. This permits the upstream influence of the inlet flowfield to distort the local dynamic pressure field at the screen planes, which in turn can cause flow distortions in the inlet and test section downstream.

Results

The results of the presented technique were compared to experimental data taken from a typical screened subsonic wind tunnel inlet.¹ Since the theoretical method is two-dimensional, an equivalent geometry based on equivalent areas was used to model the inlet.¹ Figure 1 compares measured (pressure belt) and predicted wall pressure data. This method predicted the wall pressures well, which is indicated in the figure. Test section total pressure distortions were also predicted well when a corrected screen porosity was used to account for losses in the

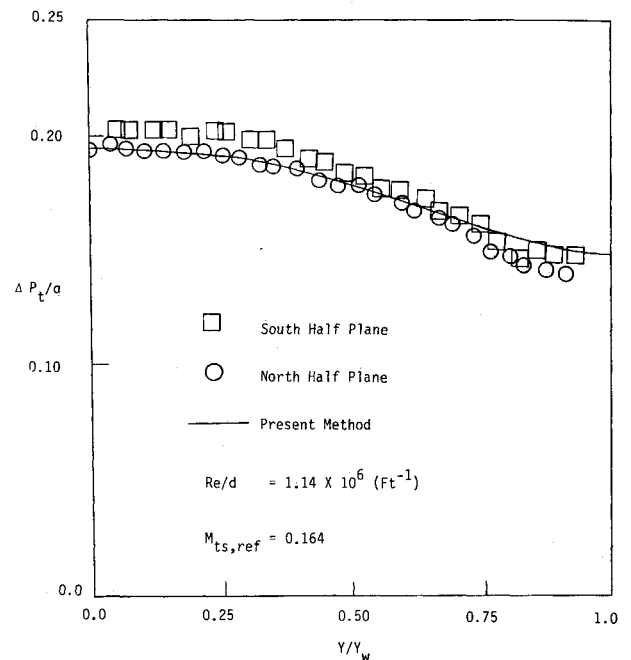


Fig. 2 Measured and predicted test section total pressure distributions.

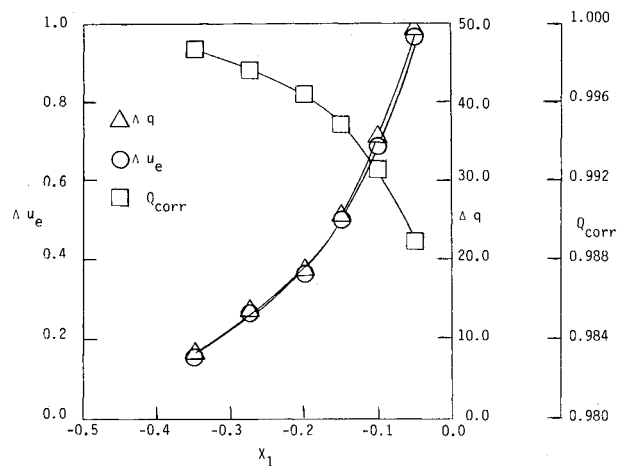


Fig. 3 The effect of screen placement on test section flow uniformity.

tunnel settling chamber not attributable to the turbulence screens.¹ This comparison to experimental pressure probe data is shown in Fig. 2. This figure indicates that the total pressure distortion from centerline to wall can be predicted well using this method.

A numerical study was undertaken to determine the effect of screen placement on test section flow quality for the tunnel under evaluation. The screen set (four screens, $\beta = 0.648$, spaced 0.05 inlet lengths apart nominally beginning 0.05 inlet lengths upstream of the inlet plane) was placed at locations successively farther upstream of the inlet plane to show the effect of screen placement on the two parameters characterizing the test section flow quality. These two parameters, Q_{corr} and Δu_e (in percent), indicate the test section dynamic pressure q and velocity u uniformity, where

$$Q_{corr} = \frac{q_{avg}}{q_{wall}} \quad (15)$$

$$\Delta u_e = \left(\frac{u_{emax} - u_{emin}}{u_{avg}} \right) \times 100 \quad (16)$$

To characterize the distortion of dynamic pressure in the plane of the leading screen, another parameter, Δq (in percent), was evaluated as follows:

$$\Delta q = \left(\frac{q_{\max} - q_{\min}}{q_{\text{avg}}} \right) \times 100 \quad (17)$$

where the leading screen is considered to be the screen closest to the inlet plane. Figure 3 shows the effect of screen placement on test section flow quality, where x_1 is the leading screen location normalized by the inlet length. This figure illustrates the improved test section flow quality with placement of turbulence-management devices further upstream of the inlet, in a flow regime of lowered inlet-induced dynamic pressure distortions.

Conclusions

A method to predict two-dimensional subsonic wind tunnel inlet flowfields based on elliptic grid generation has been developed. This method can predict the inlet and test section velocity and total pressure fields routinely for inlets containing turbulence screens. Existing elliptic grid generation codes could be readily modified to attain this capability by evaluating the source term to model the effect of the turbulence screens on the total head distribution.

References

- ¹Coirier, W.J., "A Computational Method for the Analysis of Low Speed Wind Tunnel Inlets with Screens Using an Application of Elliptic Grid Generation," Master's Thesis, Dept. of Aeronautical and Astronautical Engineering, Ohio State University, Columbus, March 1985.
- ²Wieghardt, K.E.G., "On the Resistance of Screens," *The Aeronautical Quarterly*, Vol. 17, 1953, pp. 186-192.
- ³DeVahl, D.G., "The Flow of Air Through Wire Screens," *Hydraulics and Fluid Mechanics*, Pergamon, New York, 1964, pp. 191-192.
- ⁴Thomson, J.F., Warsi, Z.U.A., and Mastin, C.W., *Numerical Grid Generation: Foundations and Applications*, North Holland, New York, 1985.

Turbulence Structure in Microburst Phenomena

George Treviño*

Michigan Technological University,
Houghton, Michigan

Nomenclature

$A_{ij}(r, t)$	= anisotropic tensor
$C_{ij}(r, t)$	= velocity-correlation tensor
$I_{ij}(r, t)$	= isotropic tensor
L	= correlation length of anisotropic turbulence
M	= mean-flow gradient
$S_{ijl}(r, t)$	= turbulence self-interaction tensor
U_i	= fluid velocity
\bar{U}_i	= mean-flow velocity
u_i	= turbulence velocity
$f(r, t)$	= longitudinal correlation function of isotropic turbulence
$g(r, t)$	= transverse correlation function of isotropic turbulence

$k(r, t)$	= arbitrary function of isotropic turbulence self-interaction tensor
σ	= turbulence intensity
Λ	= isotropic integral scale
$\Delta\Lambda$	= change in integral scale due to anisotropy

Introduction

It is rapidly becoming evident that knowledge of the interplay between turbulence and the underlying mean wind is a major key to the understanding of the microburst phenomenon¹; particularly if the attendant hazards to airplane safety and performance are to be faithfully simulated in a regulated laboratory environment.² Such simulations are of cardinal importance in control-motivated pilot training.³ The question of how isotropic turbulence "scales" in a wind-shear is of primary interest, and its study duly constitutes the essence of the fundamental problem of the microburst-turbulence phenomenon. Fortunately, the equation which governs the relation between mean-wind and turbulence is well known and understood—it is the Navier-Stokes equation of hydrodynamics, and for a steady-state turbulent fluid is written as

$$\frac{\partial U_i U_i}{\partial x_i} = \nu \frac{\partial^2 U_i}{\partial x_i \partial x_i}$$

Here U_i is the total flow, decomposing as $U_i = \bar{U}_i + u_i$, and pressure-forces have been neglected. Typically this equation is supplemented by the conservation of mass condition, $\partial U_i / \partial x_i = 0$, which also decomposes as $\partial \bar{U}_i / \partial x_i = 0$ and $\partial u_i / \partial x_i = 0$.

In the present endeavor, the effect on turbulence of a variable mean wind along the flight path of an aircraft is modeled and analyzed (see Fig. 1). The depicted headwind-to-tailwind swing is not at all uncommon in a scenario where an aircraft encounters a microburst as it is attempting to land in a thunderstorm (see Fig. 2). The accompanying variability in the mean aerodynamic lift is well-documented; but the effect of the ever-present turbulence, since its statistical characteristics are still somewhat unresolved, is a question for continued research. The following attempts to address this issue.

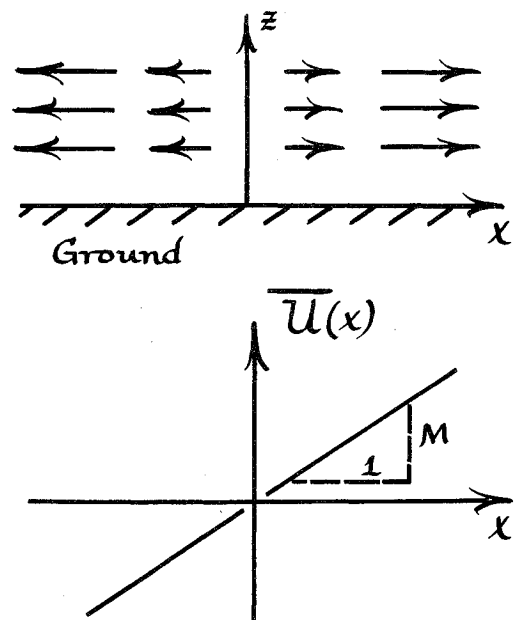


Fig. 1 Variable headwind or tailwind with velocity-gradient M .